Acta Mech. Sin. (2011) 27(6):1071–1080
DOI 10.1007/s10409-011-0511-3

RESEARCH PAPER

Adhesion behavior of endothelial progenitor cells to endothelial cells in simple shear flow

Xiao-Bo Gong[Δ] · **Yu-Qing Li**[Δ] · **Quan-Chao Gao** · **Bin-Bin Cheng** · **Bao-Rong Shen** · **Zhi-Qiang Yan** · **Zong-Lai Jiang**

[Δ] These authors contributed equally.

Received: 3 May 2011 / Revised: 17 June 2011 / Accepted: 23 June 2011

Abstract The adhesion of endothelial progenitor cells (EPCs) on endothelial cells (ECs) is one of the critical physiological processes for the regenesis of vascular vessels and the prevention of serious cardiovascular diseases. Here, the rolling and adhesion behavior of EPCs on ECs was studied numerically. A two-dimensional numerical model was developed based on the immersed boundary method for simulating the rolling and adhesion of cells in a channel flow. The binding force arising from the catch bond of a receptor and ligand pair was modeled with stochastic Monte Carlo method and Hookean spring model. The effect of tumor necrosis factor alpha (TNF-α) on the expression of the number of adhesion molecules in ECs was analyzed experimentally. A flow chamber system with CCD camera was set up to observe the top view of the rolling of EPCs on the substrate cultivated with ECs. Numerical results prove that the adhesion of EPC on ECs is closely related to membrane stiffness of the cell and shear rate of the flow. It also suggests that the adhesion force between EPC and EC by P-selectin glycoprotein ligand-1 only is not strong enough to bond the cell onto vessel walls unless contributions of other catch bond are considered. Experimental results demonstrate that TNF-α enhanced the expressions of VCAM, ICAM, P-selectin and E-selectin in ECs, which supports the numerical results that the rolling velocity of EPC on TNF-α treated EC substrate decreases obviously compared with its velocity on the untreated one. It is found that because the adhesion is affected by both the rolling velocity and the deformability of the cell, an optimal stiffness of EPC may exist at a given shear rate of flow for achieving maximum adhesion rates.

Keywords Endothelial progenitor cell · Endothelial cell · Cell adhesion · Flow chamber · Immersed boundary method

The project was supported by the National Natural Science Foundation of China (10732070, 11072155), and Shanghai Pujiang Program (09PJ1405800).

X.-B. Gong · Y.-Q. Li · B.-B. Cheng · B.-R. Shen · Z.-Q. Yan · Z.-L. Jiang (✉)
Institute of Mechanobiology and Biomedical Engineering,
School of Life Sciences and Biotechnology,
Shanghai Jiao Tong University,
200240 Shanghai, China
e-mail: zljiang@sjtu.edu.cn

X.-B. Gong · Q.-C. Gao
Department of Engineering Mechanics,
School of Naval Architecture,
Ocean and Civil Engineering,
Shanghai Jiao Tong University,
200240 Shanghai, China

1 Introduction

Increasing evidence indicates that disruption of structural and functional integrity of endothelium plays a pivotal role in the pathogenesis of cardiovascular diseases such as atherosclerosis [1, 2]. When the integrity of endothelium on vessel walls is severely disturbed, an emerging regeneration by surrounding mature endothelial cells and circulating EPCs are highly required [3, 4]. Endothelial progenitor cells (EPCs) is a special sub-type of progenitor cells in bone marrow and peripheral blood of adults, which is able to differentiate into endothelial cells (ECs) [5]. It has been proved by experiments in vivo that EPCs are important for the regenesis and angiogenesis of endothelium [6]. Clinical studies using EPCs for revascularization also suggests its great potential as a novel therapeutic option [7–9].

The endothelial repair with EPCs is a multi-step process that includes recruiting, rolling, adhesion, migration and differentiation. These processes are coupled with hemodynamics which makes the re-endothelialization more complex for involving both biofluid mechanics and mechanobiology. The migration of EPC to the injured location with binding and adhesion is critical which requires the formation of adhesive bonds between EPCs and ECs in both the extra- and intravascular space [10]. Some adhesion molecules have been implicated in the release of hematopoietic stem cells into the systemic circulation [11, 12]. Since the number of circulating EPCs in cardiovascular system is rather low [13], the adhesion mechanisms of EPCs for its enforcement has become an important area to investigate [14, 15].

For the study of coupling fluid mechanics with mechanotransduction of cells in vitro, flow chamber has been demonstrated as a simple but useful tool to use. The polymorphonuclear leukocyte rolling and adhesion was studied intensively with flow chamber by Dong et al. [16, 17] as examples. These researchers have demonstrated that cells must undergo a sequence of distinct adhesion steps to accumulate in a tissue [18, 19]. Most adhesions are initiated by a primary tethering event through selectins and their carbohydrate ligands, which allows cells to roll slowly along the vessel wall. When a rolling cell encounters a chemoattractant which binds to surface receptors, an intracellular signaling cascade is triggered to induce the functional upregulation of integrins. Integrins then bind to endothelial counter receptors for a firm arrest, here as an initial step in the sequence of repairing damaged arteries [20]. In this study, the effects of shear rates and the expression of number of adhesive molecules on rolling and adhesion of EPCs were investigated with a flow chamber system.

From the mechanical point of view, the selectin-mediated cell rolling and adhesion was modeled and nominated as adhesion dynamics since Dembo et al. [21], in which a set of constitutive equations relating stress and strain of catch bonds, and chemical rate constants of adhesion molecules to bond strain were proposed. In the recent decades, this model has been widely used to analyze the coupling of fluid mechanics with mechanobiology of cells for cell adhesion under flow conditions. Zhu et al. [22, 23] summarized more details of the rolling and adhesion of cell mediated by catching bonds of molecules. Based on these fundamental understandings, the rolling and adhesion of cells were intensively simulated [24–26]. However, in these simulations, cells were idealized as a hard sphere without deformation. Although the balances of forces and torques on cell were well accounted for, the deformation of cell which also affects the hydrodynamic shear and receptor-ligand bond formation was ignored.

Recent developments on the modeling of fluid-structure interactions have made the simulation of the deformation of cells more accessible. In this field, the particle method, hybrid lattice–Boltzmann Lagrangian method, arbitrary Lagrangian–Eulerian finite element method, boundary-integral method and the immersed boundary method have proven to be useful [27]. Using the immersed boundary method [28, 29], Jadhav et al. [30] analyzed how cell deformation affects selectin-mediated leukocyte rolling, in which the effects of mechanical properties of the cell were investigated. Pappu et al. [31] also employed the same method and studied the adhesion of leukocyte in microvessels and its effect on flow patterns.

In this paper, the very early stage of EPC repair in which rolling and adhesion of an EPC on EC substrate occurred was studied numerically in association with some relevant experiments. The fluid dynamics and the adhesion dynamics were coupled for a comprehensive understanding of the EPC-EC adhesion. The effects of TNF-α on molecular expression and enhancement of adhesion force were also investigated.

2 Computational methods

2.1 Fluid-structure interaction with the immersed boundary method

The adhesion behavior of an EPC on EC substrate in a simple shear flow was modeled in a two-dimensional context based on the immersed boundary method. The motion of cell immersed in an incompressible fluid was described with a single set of Navier–Stokes equation as

$$\nabla \cdot \boldsymbol{u} = 0, \tag{1}$$

$$\rho\left(\frac{\partial \boldsymbol{u}}{\partial t} + \boldsymbol{u} \cdot \nabla \boldsymbol{u}\right) = -\nabla p + \nabla \cdot \mu(\nabla \boldsymbol{u} + \nabla \boldsymbol{u}^{\mathrm{T}}) + \boldsymbol{F}, \tag{2}$$

where $\boldsymbol{F}$ denotes the source term of fluid-membrane interaction force $\boldsymbol{f}_{\mathrm{e}}$ which comes from the deformation of cell membrane, and the adhesion force on the membrane $\boldsymbol{f}_{\mathrm{a}}$ due to catch bonds formation of adhesive molecules. Two separated grid systems were used in the immersed boundary method. Navier–Stokes equation for the whole flow field was discretized and solved on a stationary grid; and the other was an unstructured grid, triangular element in this study, which was movable and deformable for representing the interface. Here, a delta function was used for communicating the forces arising on the membrane $\boldsymbol{f}$ and in the Navier–Stokes equation $\boldsymbol{F}$ as

$$\boldsymbol{F}(\boldsymbol{x}, t) = \int_{\Gamma} \boldsymbol{f}(\boldsymbol{x}', t)\delta(\boldsymbol{x} - \boldsymbol{x}')\mathrm{d}l, \tag{3}$$

where Γ is the length of cell, $\boldsymbol{x}$ and $\boldsymbol{x}'$ stand for the coordinates on the stationary grids and the unstructured grids, respectively. After the Navier–Stokes equation was solved on the stationary grid, the velocity was interpolated onto the nodes of unstructured grid as

$$\boldsymbol{u}(\boldsymbol{x}', t) = \int_{S} \boldsymbol{u}(\boldsymbol{x}, t)\delta(\boldsymbol{x} - \boldsymbol{x}')\mathrm{d}s. \tag{4}$$

The unstructured grid was then tracked in a Lagrangian way as

$$\boldsymbol{x}'_t = \boldsymbol{x}'_0 + \int_0^t \boldsymbol{u}(\boldsymbol{x}', t)\mathrm{d}\tau. \tag{5}$$

The stress in the membrane accompanied with the deformation and adhesion was firstly calculated on the unstructured grid, then distributed onto the stationary grid with the distribution function given by Tryggvason et al. [29]

$$D(\boldsymbol{x} - \boldsymbol{x}') = \begin{cases} (4h)^{-n} \prod_1^n \left[1 + \cos\dfrac{\pi}{2h}(\boldsymbol{x} - \boldsymbol{x}')\right], & |\boldsymbol{x} - \boldsymbol{x}'| < 2h, \\ 0, & \text{otherwise}, \end{cases} \tag{6}$$

where h is the grid size; n indicates the spatial dimensions, and $n = 2$ in the present work. With this utilization of discretized delta function, Eqs. (3) and (4) were used in the present work as

$$\begin{aligned} \boldsymbol{F}(\boldsymbol{x}_i) &= \sum_j \boldsymbol{f}(\boldsymbol{x}'_j) D(\boldsymbol{x}_i - \boldsymbol{x}'_j), \\ \boldsymbol{u}(\boldsymbol{x}'_i) &= \sum_j \boldsymbol{u}(\boldsymbol{x}_j) D(\boldsymbol{x}_j - \boldsymbol{x}'_i). \end{aligned} \tag{7}$$

2.2 EPC modeling

Owing to the lack of known mechanical properties of EPC, the effect of the whole elasticity of the cell on its rolling and adhesion behavior has been considered in two ways in this paper. One is the shear modulus of the membrane. The other is a higher viscosity for the fluid inside the cell than the outside to account for the effects of nucleus and inner cytoskeletal structures of the cell. Briefly, EPC was modeled as a viscous liquid surrounded by a hyper-elastic membrane [32, 33]. The hyper-elastic membrane proposed by Skalak et al. [34] was adopted.

Since a two-dimensional membrane was considered here, the stress was calculated as the membrane stretched in one principal direction only [35, 36] with the assumption that on the other principal direction, the in-plane stress equals zero. Here

$$\tau_1^{\mathrm{SK}} = B\lambda_1(\lambda_1^2 - 1)\sqrt{\frac{1 + C\lambda_1^2}{1 + C\lambda_1^4}}\left(\frac{1 + C\lambda_1^4}{1 + C\lambda_1^2} + \frac{C}{1 + C\lambda_1^4}\right), \tag{8}$$

where λ_1 is the principal strain; B and C are the shear coefficient and the surface dilation coefficient of the membrane, respectively. Related studies by Gong et al. [27] and Pozrikidis et al. [37] showed that for Skalak model, the surface dilation coefficient is less sensitive and the stiffness of the cell is affected mainly by its shear modulus. Three different values of shear modulus for membrane modeling, $3.0\,\mu$N/m, $12\,\mu$N/m and $24\,\mu$N/m were adopted. When the shear modulus reaches $24\,\mu$N/m, it is almost as stiff as a leukocyte membrane [38]. The bending stiffness was considered by introducing a bending force, q, as $q = \mathrm{d}m/\mathrm{d}l$, $m = E_{\mathrm{B}}(\kappa - \kappa_{\mathrm{R}})$. Here m is the bending moment, E_{B} is the bending modulus, l is the length of the elements of the cell, κ and κ_{R} are the local curvature and the curvature at resting configurations of the cell, respectively.

Following Pozrikidis [32], the jump in hydrodynamics traction across the cell membrane was expressed by counting the in-plane stress and the bending stiffness of the cell as

$$\boldsymbol{f}_{\mathrm{e}} \cdot l = (\tau_i \boldsymbol{t}_i - \tau_j \boldsymbol{t}_j) + (q_i \boldsymbol{n}_i - q_j \boldsymbol{n}_j), \tag{9}$$

where the subscript "i" and "j" denote the number of the elements and the force $\boldsymbol{f}_{\mathrm{e}}$ is given on the node shared by i and j element; $\boldsymbol{t}$ and $\boldsymbol{n}$ represents the tangential and normal unit vectors of the elements; τ and q represents the in-plane stress and the bending stress, respectively.

2.3 Stochastic Monte Carlo method for receptor-ligand interactions

The adhesion force represented by the interaction between a receptor and ligand pair was modeled by Hookean spring as

$$\boldsymbol{f}_{\mathrm{a}}(\boldsymbol{x}') = k_{\mathrm{b}}(l - l_0)\boldsymbol{n}, \tag{10}$$

where k_{b} is the spring constant which stands for the elasticity of the bonds formed by the receptor and ligand pair, l and l_0 are the stretched and un-stretched length of the bonds, $\boldsymbol{n}$ is the normal unit vector of the membrane at the point of bond formation.

According to Dembo [21], the forward and reverse rate constants for receptor-ligand interactions under external force were computed as

$$\begin{aligned} k_{\mathrm{f}} &= k_{\mathrm{f}}^0 \exp\left[-\frac{k_{\mathrm{ts}}(l - l_0)^2}{2K_{\mathrm{B}}T}\right], \\ k_{\mathrm{r}} &= k_{\mathrm{r}}^0 \exp\left[\frac{(k_{\mathrm{b}} - k_{\mathrm{ts}})(l - l_0)^2}{2K_{\mathrm{B}}T}\right]. \end{aligned} \tag{11}$$

Here, k_{f} and k_{r} are the forward and reverse reaction rates, respectively. k_{ts} is the spring constant of the bond at transition state, K_{B} is the Boltzmann constant, and T is the absolute temperature.

Following Bhatia et al. [39], Jadhav et al. [30] and Pappu et al. [31] in their simulations of leukocyte adhesion, used stochastic Monte Carlo method to simulate the formation of receptor/ligand bonds between the moving EPC and EC substrate. In a given time interval Δt, the probability of the formation of a new bond P_{f}, and that of the rupture of an existing bond P_{r} were given as

$$\begin{aligned} P_{\mathrm{f}} &= 1 - \exp(-k_{\mathrm{f}}\Delta t), \\ P_{\mathrm{r}} &= 1 - \exp(-k_{\mathrm{r}}\Delta t). \end{aligned} \tag{12}$$

To realize the stochastic Monte Carlo process numerically, two random numbers between 0 and 1, say N_1 and N_2, were generated independently at each time step. A new bond is allowed to form if $P_{\mathrm{f}} > N_1$, and an existing bond is allowed to rupture if $P_{\mathrm{r}} > N_2$. When the number of adhe-

sive molecules on EC substrate increases because of TNF-α treatment, the possibility of P_f increases correspondingly. Similarly, the adhesion force also increases as the number of adhesive molecular bonds increases.

All the receptor/ligand interaction were firstly checked by the algorithm following stochastic Monte Carlo process, and the forces were first calculated from Eq. (10) on the membrane, then distributed onto the flow field, similar to the treatment of the stress of membrane deformation following Eq. (3). In the present simulation of catch bonds dynamics, the effect of diffusion of receptors/ligands after bond formation/rupture was not considered.

2.4 Numerical simulation schemes

The numerical schemes for solving Navier–Stokes equation [27, 33] are summarized briefly as follows. The coupling of continuity and momentum was solved using the fractional step of marker and cell (MAC) method. The second-order central difference scheme was used for both the convection and viscous terms. The second-order Adams–Bashforth scheme was used for the time integration. The second-order Crank–Nicolson method was used for the viscous term for managing larger time step. Periodic boundary conditions were used for the inlet and outlet of the flow. Non-slip boundary and Neumann conditions were adopted for wall boundaries of velocity and pressure, respectively. The present method for simulating cell deformation in channel flow and shear flow was validated as did in the previous works [27, 33] and omitted here.

3 Experimental materials and methods

A flow chamber system was set up for comparison with simulation results. Effects of TNF-α on the molecular expression and enhancement of adhesion force was also investigated with molecular experiments. The experimental protocols are summarized briefly here.

3.1 Isolation and identification of EPCs and ECs

Human blood mononuclear cells were isolated from cord blood by density gradient centrifugation with Ficoll-Paque Plus (Cedarlane Canada). The isolated cells were incubated with Medium 199 (Gibco-BRL, Grand Island, NY) essential medium, supplemented with 20 % fetal-calf serum (Gibco-BRL, Grand Island, NY), human aFGF, bFGF, (5 ng/ml, Sigma, Saint Louis) etc., in tissue culture plates at 37°C and 5 % CO_2. Three days after seeding, non-adherent cells were removed by washing with phosphate-buffer saline (PBS). The adherent cells were used as target cells in later experiments.

ECs were isolated from fresh human umbilical veins using the collagenase perfusion technique. Briefly, ECs were harvested from the vein by adding 0.1 % collagenase for 12 minutes. The cells were cultured in medium 199 Earle (Gibco, Grand Island, NY) containing 20 % heat-inactivated fetal bovine serum (FBS; Gibco), 100 mmol HEPES (Sigma, Saint Louis), 100 U/ml penicillin, 100 mg/ml streptomycin, 2 mmol glutamine, 5 ng/ml aFGF (Sigma) and 5 U/ml heparin (Sigma). ECs were cultured to confluence in 25 cm^2 culture flasks (Costar, NY). Cells were assessed for EC phenotype by morphology, typical monolayer cobblestone growth pattern, and expression of von Willebrand factor antigen (DukoCytomation, Glostrup, Denmark). ECs between Passages 1 and 3 were used in all experiments.

3.2 Cell adhesion assay under flow conditions

The flow chamber system consists of a square glass tube, a syringe pump and a CCD camera (CCD-72, Dage-MTI Inc., Michigan City, Indiana) attached to the microscope (Olympus IX71) for observation.

A square glass tube with a cross section of 1 mm by 1 mm and 80 mm in length was used. ECs, either activated by incubation with TNF-α (10 ng/ml; Sigma) for 6 hours or inactivated, were seeded on the bottom of the glass tube. For a comparison, the rolling of EPCs on the substrate of glass tube without EC seeded was also observed. Syringes filled with EPC suspension were pushed into the flow chamber which was mounted on the stage of the inverted fluorescence microscope. The velocity of EPCs was recorded. Here, the flow rate of syringe pump was controlled to form a shear rates from 10 to 40/s, which was limited by the frame rate of CCD camera (3 frames per second). The images were recorded with the software Image-Proplus 6.3. It was observed that the averaged cell rolling velocity was recorded at the time scale of the order of seconds although fluctuations in the velocity may be of the order of mini-seconds when affected by the formation and rupture of catch bonds.

3.3 Cell adhesion molecular assay (western blotting assay)

To detect the protein expression of EC adhesion molecules under TNF-α stimulation, ECs were seeded into the bottom of glass tube at a density of 6×10^5 cells and cultured to achieve confluent monolayers. ECs were then treated with TNF-α (10 ng/ml; Sigma) for 6 hours. Inactivated ECs without TNF-α treatment was adopted as a control group. Protein samples after washing with PBS was collected and Western blot analysis was performed following the protocols described by Qi et al. [40]. EC protein lysates were subjected to electrophoretic separation with 10% SDS-PAGE and transferred to nitrocellulose membranes (Hybond, Amersham). The proteins were detected using specific primary antibodies for VCAM (1:1 000, Santa Cruz Technology, INC), ICAM (1:800, Santa Cruz Technology, INC), E-selectin (1:200, Boster), P-selectin (1:200, Boster) and GAPDH (1:500, Santa Cruz Technology, INC).

4 Results and discussions

The adhesive molecules of catch bonds between EPCs and ECs has yet to be quantitatively evaluated [41], therefore, the most commonly involved adhesive bonds of P-selectin Glycoprotein Ligand-1 (PSGL-1) was chosen. Relative coefficients used in the present work for adhesion dynamics modeling were summarized in Table 1.

Table 1 Parameters used in the present work for EPC adhesion simulation

Parameters	Value	References
EPC diameter/μm	20.0	Measured by experiments
Channel height/μm	80–100	
Shear rate/s^{-1}	80–1 200	
Length of microvillus/μm	0.35	Shao et al. [42]
Number of microvillus/cell	252	Chen and Springer [43]
Number of ligands per microvilli	50	Moore et al. [44]
Receptor site density/μm^2	150	Yago et al. [45]
Receptor-ligand bond length/μm	0.1	Marshall et al. [46]
Spring constant (k_b)/(pN·nm^{-1})	1	Marshall et al. [46]
Transition spring constant (k_{ts})/(pN·nm^{-1})	0.99	Smith et al. [47]
Unstressed on rate/s^{-1}	1	Mehta et al. [48]
Unstressed off rate/s^{-1}	1	Mehta et al. [48]

Nondimensionalization of the parameters were performed in this study. The time t^* and length L^* scales were the invert of shear rates and the average diameter of EPC, respectively. The results were presented and discussed as follows.

The EPC profiles changing with time in the channel were shown in Fig. 1, in which the effect of stiffness of cell membrane, and the shear rates of the channel flow on the rolling velocity of cell were presented. The fixed marker on the membrane of EPC helps to illustrate that the cells in the channel were rolling with sliding along the bottom. Since there was no parallel forces acting on the cell which would push the cell to the channel wall, cells tended to migrate to the center of the channel due to the lubrication effect of flow. Figure 1a showed that when the cell membrane became stiffer, the rolling velocity decreased and the resistance, i.e. the apparent viscosity of the flow in channel increased. A comparison of cell profiles at the same stiffness but exposed to different shear rates is shown in Figs. 1b and 1c series, which suggests that with the increase of the shear rate, cells underwent larger deformation in the flow field, which helped the formation of catch bonds since the average distance between the EPC membrane and the substrate of ECs decreased. It also showed that with the increase of stiffness, cells tended to migrate slower to the center of the flow field because of their smaller deformability.

The profiles of the cells suffering the same shear rate but with different membrane stiffnesses and the number of adhesive molecules were compared in Fig. 2. The results suggested that with the increase of cell stiffness, EPCs tended to retard by the adhesion, while the softer cells were more amenable to migrate away from the vessel wall. When cells moved slower, they tended to have more time to form catch bonds after they were initially released near the vessel wall. Figure 2 also shows that in most of the cases in which only the adhesion force associated with bonds of PSGL-1 was considered, the force was not high enough to capture EPCs near the vessel wall region.

The top view of an EPC rolling on the substrate seeded with ECs in the flow chamber is illustrated in Fig. 3. In order to classify that the cell rolling in the view point was EPC, the carboxymethyl (CAM) was used as a fluorescence marker as shown in Fig. 3c. As presented in Sect. 3.2, the frequency of the camera used in the present work is too low to catch the adhering, tethering and rupture process which is of the order of mini-seconds in the time scale. However, according to the cell rolling velocity observed of the order of seconds, there were still noted differences arising from different shear rates of the flow. Especially after ECs were treated by TNF-α, the rolling velocity of EPCs on it became significantly slower than that of EPC rolling on normal ECs.

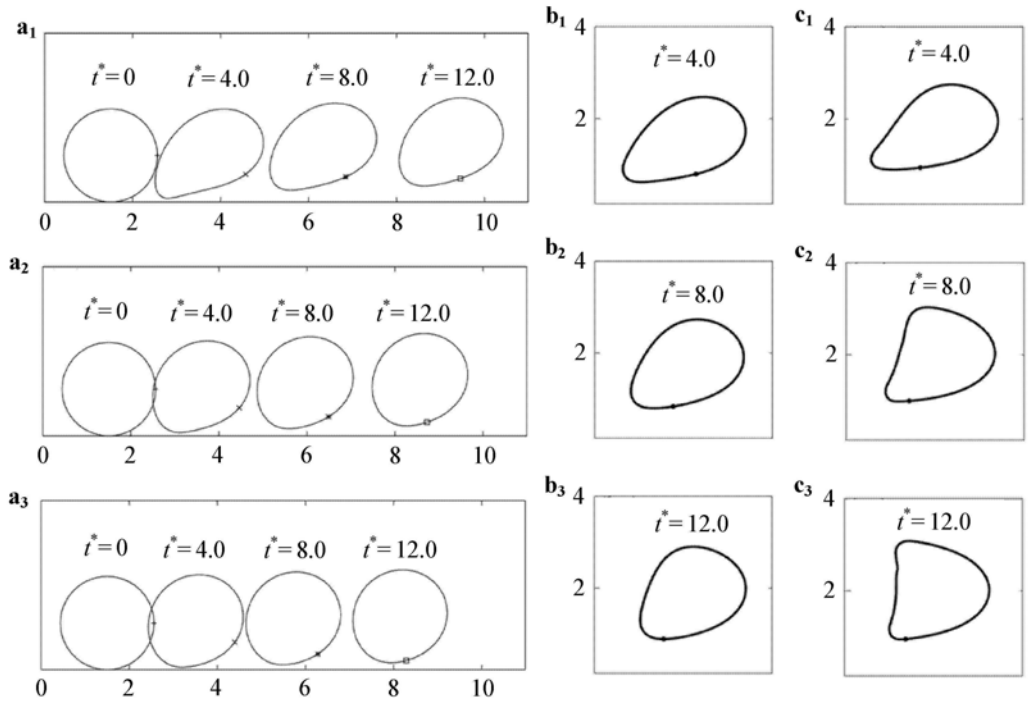

Fig. 1 Profiles of rolling cells at different shear moduli of the membrane without adhesion force. The dot on the ring of cell stands for the same point which illustrates of tank-treading motion of the membrane while cell rolls and moves forward. For series **a**, $\dot{\gamma} = 83.3$, $\mathbf{a}_1$ $B = 3.0\,\mu$N/m; $\mathbf{a}_2$ $B = 12.0\,\mu$N/m; $\mathbf{a}_3$ $B = 24.0\,\mu$N/m. For series **b**, $\dot{\gamma} = 250$ and $B = 3.0\,\mu$N/m. For series **c**, $\dot{\gamma} = 583.1$ and $B = 3.0\,\mu$N/m

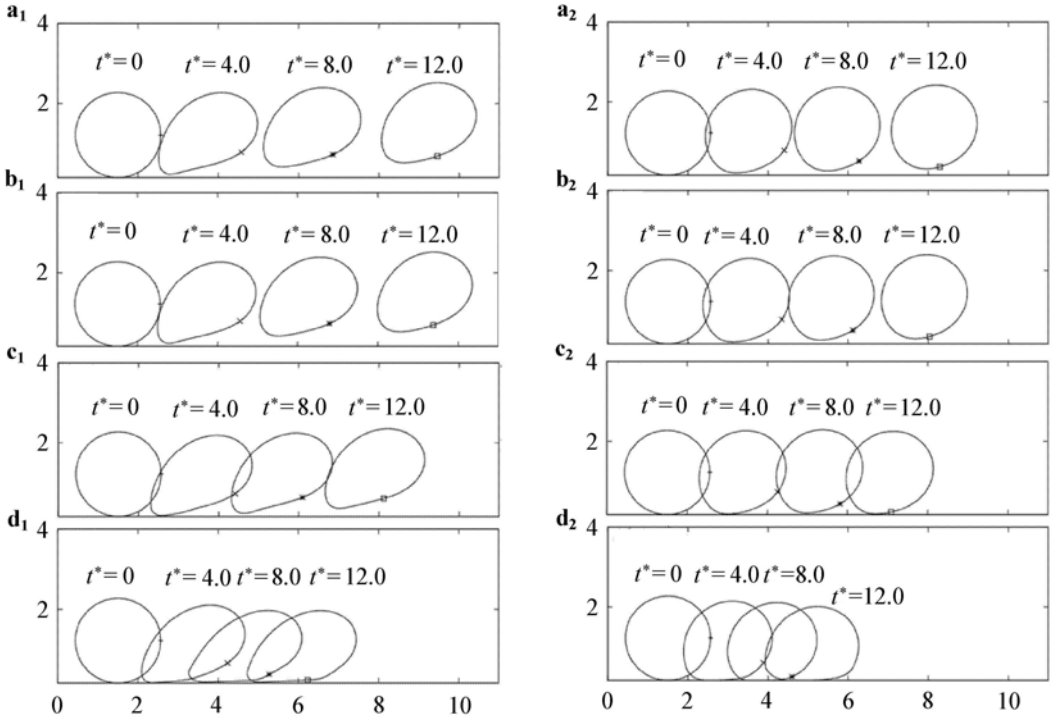

Fig. 2 Profiles of rolling cells with different adhesion effects at $\dot{\gamma} = 83.3$. **a** Flow without adhesion; **b** Flow with normal adhesion; **c** Adhesion with TNF affected and 2 times of adhesion molecular expressed; **d** TNF-α affected with 10 times of adhesion molecular expressed. For the columns on the left side $B = 3.0\,\mu$N/m. For the columns on the right side $B = 24.0\,\mu$N/m

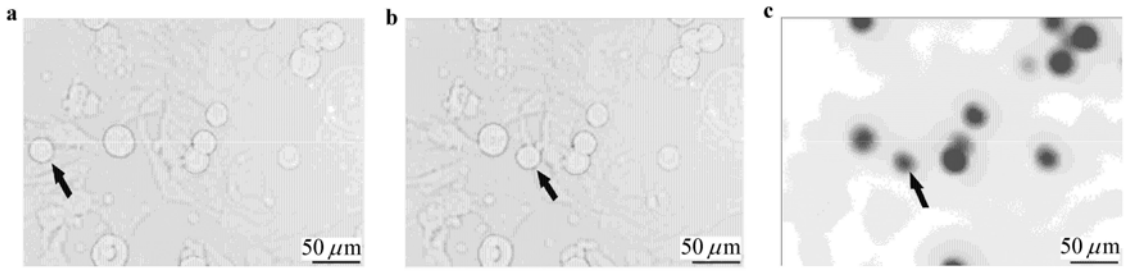

Fig. 3 The rolling process of EPC captured. **a** The start point of EPC rolling; **b** The terminal point of EPC rolling; **c** The terminal point of EPC rolling labeled by CAM. The arrows show the target rolling cell

When the adhesion force is taken into account, the development of cell rolling velocity at different shear moduli of the cell is shown in Fig. 4. The on-off of the catch bonds affected the rolling of EPCs so that there appeared sudden acceleration and deceleration of the cell. The detailed evolution of velocity profile suggests that if the unique catch bonds of PSGL-1 is not strong enough to catch an EPC to EC substrate, a steady rolling process was observed as illustrated in Fig. 2. Figure 4 also shows that the stiffer the EPC, the higher the probability of adhesion of cell, and the slower the rolling velocity of cell.

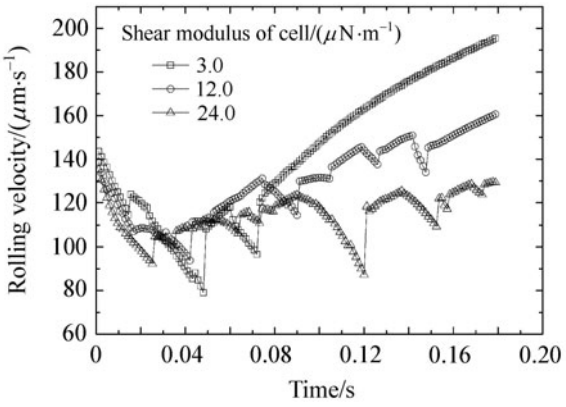

Fig. 4 Numerical results of the history of rolling velocity at $\dot{\gamma} = 83.3$ with different shear moduli of the membrane in which the adhesion effects are considered by the stochastic Monte Carlo method

For studying the effect of numbers of adhesive molecules on rolling and adhesion of EPC, TNF-α treatment of EC substrate was performed. TNF-α is a type of cytokine produced from the macrophage cell activated. It is the most robust cell factors for antineoplastic activity that is related to the adhesion, migration and several other functions of cells. Dudeck et al. [41] proved by experiments that TNF-α promotes the expression of VCAM-1, P-selectin and E-selectin of ECs, so that the adhesion between bone marrow-derived cultured mast cell and ECs is enhanced. Here, experiments following the protocol in Sect. 2.4 were performed to enhance the expression of adhesive molecules on ECs. Four typical adhesive molecules of ECs, VCAM-1, ICAM-1, P-selectin and E-selectin, after TNF-α treatment were examined by Western plot analysis as shown in Fig. 5. It is shown that compared with the control group, the adhesion molecules were increased apparently from 33 % to almost 100 % after TNF-α treatment.

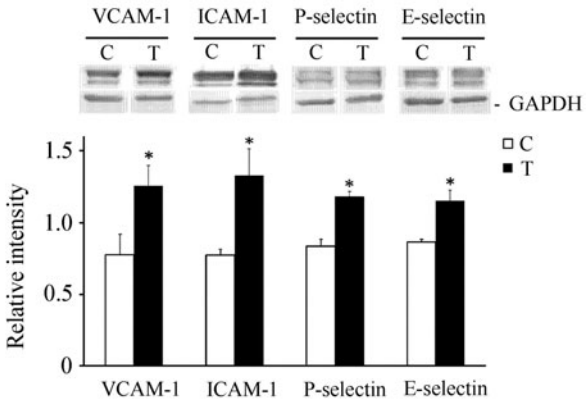

Fig. 5 TNF-α increased the expressions of adhesion molecules, VCAM, ICAM, P-selectin and E-selectin, in ECs cultured on the bottom of the glass tube. Western blot analysis showing values of protein amounts were normalized to GAPDH expression. Group C is that ECs cultured with EC complete medium only, without any TNF-α treatment; Group T is that treated with TNF-α at 10 ng/ml for 6 hours. The data from four independent experiments are shown as mean $\pm SD$, $^{*}p < 0.05$, $n = 4$

The effects of stiffness of cell and the flow shear rate on the rolling velocity of EPCs were shown in Fig. 6. The differences of cell rolling velocity at different cell stiffnesses increased with increase in shear rate (Fig. 6). The results suggested that deformability of cell is one of the key parameter for successful adhesion, but this could not be uniformly summarized in a simple way for various shear rates of the flow. The increase of cell deformation helps to enlarge the contact area (contact line in two-dimensional cases) between the cell and the substrate of the flow chamber, which increases the possibility of bond formation and the adhesion

forces thereby. Although the increase of stiffness slowed down the rolling velocity of cell which increased the possibility of bond formation, smaller deformability also resulted in smaller contact lines between EPC and the adhesive substrate. Figure 6 suggests that in general, the adhesion will slow down the rolling velocity of cell, but what combination of shear rate and cell stiffness will be optimal for adhesion is still a case specific problem.

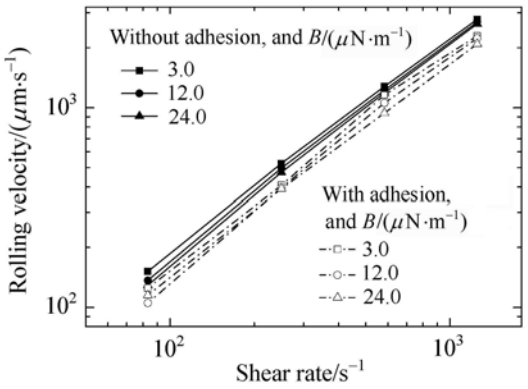

Fig. 6 Cell rolling velocity in channel flows with different shear rates and shear moduli of the cell

The increase in the amount of adhesive molecules was correlated to the possibility of bond formation through the increase of frequency for N_1 generation. For example, when the adhesive molecules was increased up to twice that of normal EC, two times of N_1 was then generated during one time interval and compared with P_f. Besides that, when a bond formation was confirmed by stochastic process, the adhesive force arising from the bond also increased proportionally due to an increase in the adhesive molecules. As shown in Fig. 7, the increase in the number of adhesive molecules resulted in the decrease in the rolling velocity. The increase of adhesion force for the cell at a shear modulus of 12 μN/m seems to be the optimal one compared with softer and stiffer cells. This is because the adhesion force is affected by the combination of both cell rolling velocity and its deformability as analyzed above.

The history of adhesion force in the early stage of EPC rolling on EC substrate is illustrated in Fig. 8. The increase of adhesive molecules promoted the adhesion force both in possibility and in magnitude, which suggests that stimulation of adhesion substrate is a useful way for EPC recruiting. This result is in accordance with the changes of cell rolling velocity for different molecule expressions shown in Fig. 7.

The formation rate was calculated by summing the total bond number during the time interval and divided by the time interval (Fig. 9). The result suggests that with a stiffer membrane, the bond formation rates on membrane decrease sharply with the increase in the shear rates of flow. But for softer ones, the tendency is not clear because both the deformability and the moving velocity of the cell can individually make significant contribution to bond formation.

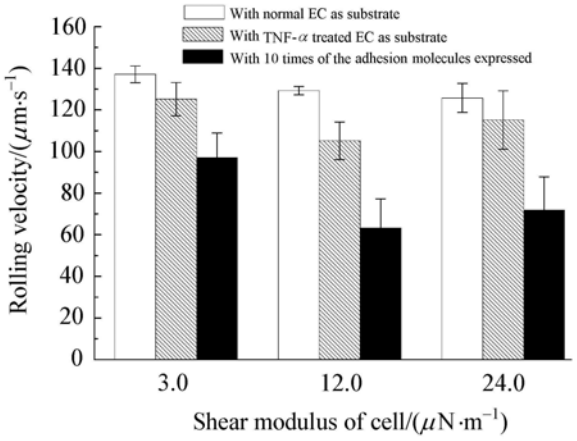

Fig. 7 Comparison of cell rolling velocity with different amount of adhesive molecules on substrate at shear rate $\dot{\gamma}$ = 83.3

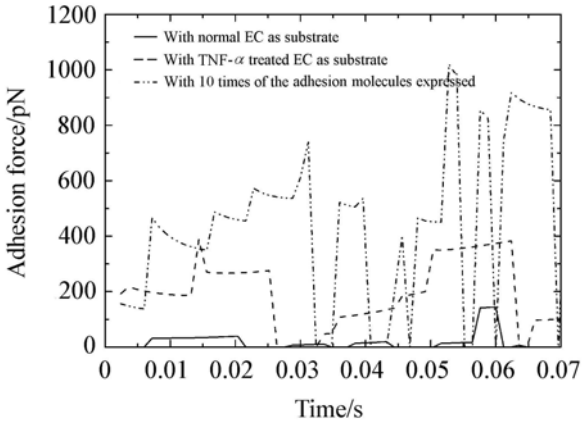

Fig. 8 Time sequence of the adhesion force with different conditions of EC substrate in the early stage of EPC adhesion at shear rate $\dot{\gamma}$ = 83.3

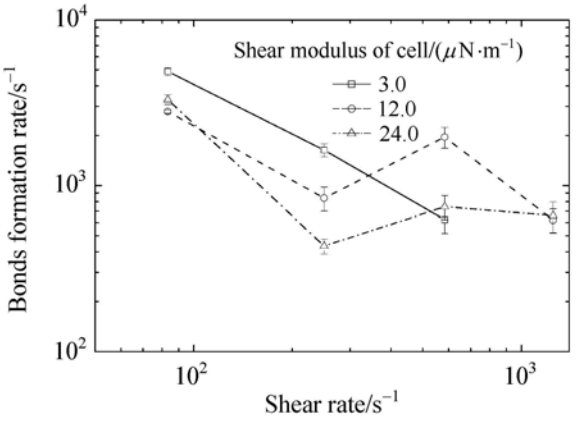

Fig. 9 Bonds formation rates with shear rate for different shear modulus of cell

5 Concluding remarks

The adhesion behavior of EPCs on ECs substrate under a simple shear flow was modeled and studied numerically. The simulation results show that both the stiffness and the shear rate of the flow are critical for the rolling and adhesion of the EPCs on ECs. When the migration force which pushes EPCs onto the vessel wall is neglected, the adhesion force from the catch bonds of PSGL-1 only is not strong enough to hold the EPCs steadily on the EC substrate. In the early stage of cell adhesion, as the adhesion force is affected by the combination of both cell rolling velocity and its deformability, an optimal stiffness of EPC may exists under a given shear rate of flow for achieving maximum adhesion probability. It is hoped that this study can not only help better understand the adhesion behavior of EPCs on ECs, which is one of the critical processes for angiogenesis, but also contribute towards the development of novel therapeutic options for cardiovascular diseases.

References

1 Hughes, S.F., Cotter, M.J., Evans, S.A., et al.: Role of leucocytes in damage to the vascular endothelium during ischaemia-reperfusion injury. Br. J. Biomed. Sci. **63**(4), 166–170 (2006)

2 Beohar, N., Rapp, J., Pandya, S., et al.: Rebuilding the damaged heart—the potential of cytokines and growth factors in the treatment of ischemic heart disease. J. Am. Coll. Cardiol. **56**, 1287–1297 (2010)

3 Huang, P.H., Chen, Y.H., Chen, Y.L., et al.: Vascular endothelial function and circulating endothelial progenitor cells in patients with cardiac syndrome X. Heart **93**(12), 1064–1070 (2007)

4 Shmilovich, H., Deutsch, V., Roth, A., et al.: Circulating endothelial progenitor cells in patients with cardiac syndrome X. Heart **93**(12), 1071–1076 (2007)

5 Asahara, T., Murohara, T., Sullivan, A., et al.: Isolation of putative progenitor endothelial cells for angiogenesis. Science **275**(5302), 964–966 (1997)

6 Hristov, M., Erl, W., Weber, P.C.: Endothelial progenitor cells: mobilization, differentiation, and homing. Arterioscler Thromb. Vasc. Biol. **23**(7), 1185–1189 (2003)

7 Urbich, C., Dimmeler, S.: Endothelial progenitor cells: characterization and role in vascular biology. Circ. Res. **95**, 343–353 (2004)

8 Oren, M.T., Robert, D.G., Jennifer, M.C., et al.: Human endothelial progenitor cells from type II diabetics exhibit impaired proliferation, adhesion, and incorporation into vascular structures. Circulation **106**, 2781–2786 (2002)

9 Dzau, V.J., Gnecchi, M., Pachori, A.S., et al.: Therapeutic potential of endothelial progenitor cells in cardiovascular diseases. Hypertension **46**(1), 7–18 (2005)

10 Xu, Q.: Endothelial progenitor cells in angiogenisis. Acta Physiol. Sin. **57**(1), 1– 6 (2005)

11 Frenette, P.S., Subbarao, S., Mazo, I.B., et al.: Endothelial selectins and vascular cell adhesion molecule-1 promote hematopoietic progenitor homing to bone marrow. PNAS **95**(24), 14423–14428 (1998)

12 Gangenahalli, G., Singh, V., Verma, Y., et al.: Hematopoietic stem cell antigen CD34: role in adhesion or homing. Stem. Cells Dev. **15**(3), 305–313 (2006)

13 Hirstov, M., Weber, C.: Endothelial progenitor cells: characterization, pathophysiology, and possible clinical relevance. J. Cell Mol. Med. **8**(4), 498–508 (2004)

14 George, J., Hertz, I., Goldstein, E., et al.: Number and adhesive properties of circulating progenitor cells in patients with in-stent restenosis. Arterioscl. Thromb. Vasc. Biol. **23**, 1–5 (2003)

15 George, J., Goldstein, E., Abashidze, A., et al.: Erythropoietin promotes endothelial progenitor cell proliferative and adhesive properties in a PI 3-kinase-dependent manner. Cardiovasc. Res. **68**, 299–306 (2005)

16 Dong, C., Cao, J., Struble, E.J., et al.: Mechanics of leukocyte deformation and adhesion to endothelium in shear flow. Ann. Biomed. Eng. **27**(3), 298–312 (1999)

17 Dong, C., Lei X.X.: Biomechanics of cell rolling: shear flow, cell-surface adhesion, and cell deformability. J. Biomech. **33**(1), 35–43 (2000)

18 Mazo, I., Gutierrez–Ramos, J., Frenette, P.S., et al.: Hematopoietic progenitor cell rolling in bone marrow microvessels: parallel contributions by endothelial selectins and vascular cell adhesion molecule 1. J. Exp. Med. **188**(3), 465–474 (1998)

19 Mazo, I., von Andrian, U.H.: Adhesion and homing of blood-borne cells in bone marrow microvessels. J. Leukoc. Biol. **66**, 25–32 (1999)

20 Ross, R.: The pathogenesis of atherosclerosis: a perspective for the 1990s. Nature **362**(6423), 801–809 (1993)

21 Dembo, M., Torney, D.C., Saxman, K., et al.: The reaction-limited kinetics of membrane-to-surface adhesion and detachment. Proc. Roy. Soc. B: Biol. Sci. **234**(1274), 55–83 (1988)

22 Zhu, C., Yago, T., Lou, J., et al.: Mechanisms for flow-enhanced cell adhesion. Ann. Biomed. Eng. **36**, 604–621 (2008)

23 McEver, R., Zhu, C.: Rolling cell adhesion. Annu. Rev. Cell Dev. Biol. **26**, 7.1–7.34 (2010)

24 Hammer, D.A., Apte, S.M.: Simulation of cell rolling and adhesion on surfaces in shear flow: general results and analysis of selectin-mediated neutrophil adhesion. Biophys. J. **63**(1), 35–57(1992)

25 Chang, K.C., Hammer, D.A.: Adhesive dynamics simulations of sialyl-lewisx/E-selectin-mediated rolling in a cell-free system. Biophys. J. **79**(4), 1891–1902 (2000)

26 King, M.R., Hammer, D.A.: Multiparticle adhesive dynamics: hydrodynamic recruitment of rolling leukocytes. PNAS **98**(26), 14919–14924 (2001)

27 Gong, X., Sugiyama, K., Takagi, S., et al.: The deformation behavior of multiple red blood cells in a capillary vessel. J. Biomech. Eng. **131**, 074504 (2009)

28 Peskin, C.: Numerical analysis of blood flows in the heart. J. Comput. Phys. **25**, 220–252 (1977)

29 Tryggvasona, G., Bunnerb, B., Esmaeelic, A., et al.: A front-tracking method for the computations of multiphase flow. J. Comput. Phys. **169**(2), 708–759 (2001)

30 Jadhav, S., Eggleton, C., Konstantopoulos, K.: A 3-D computational model predicts that cell deformation affects selectin-

mediated leukocyte rolling. Biophys. J. **88**, 96–104 (2005)
31 Pappu, V., Doddi, S.K., Bagchi, P.: A computational study of leukocyte adhesion and its effect on flow pattern in microvessels. J. Theor. Biol. **254**, 483–498 (2008)
32 Pozrikidis, C.: Effect of membrane bending stiffness on the deformation of capsules in simple shear flow. J. Fluid Mech. **440**, 269–291 (2001)
33 Takagi, S., Yamada, T., Gong, X., et al.: The deformation of a vesicle in a linear shear flow. J. Appl. Mech. **76**, 021207 (2009)
34 Skalak, R., Tozeren, A., Zarda, R., et al.: Strain energy function of red blood cell membranes. Biophys. J. **13**, 245–264 (1973)
35 Barthes-Biesel, D., Diaz, A., Dhenin E.: Effect of constitutive laws for two-dimensional membranes on flow-induced capsule deformation. J. Fluid Mech. **460**, 211–222 (2002)
36 Bagchi, P.: Mesoscale simulation of blood flow in small vessels. Biophys. J. **92**(6), 1858–1877 (2007)
37 Pozrikidis, C.: Numerical simulation of the flow-induced deformation of red blood cells. Ann. Biomed. Eng. **31**, 1194–1205 (2003)
38 Lim, C.T., Zhou, E.H., Quek, S.T.: Mechanical models for living cells—a review. J. Biomech. **39**, 195–216 (2006)
39 Bhatia, S.K., King, M.R., Hammer, D.A.: The state diagram for cell adhesion mediated by two receptors. Biophys. J. **84**, 2671–2690 (2003)
40 Qi, Y.X., Qu, M.J., Long, D.K., et al.: Rho-GDP dissociation inhibitor alpha downregulated by low shear stress promotes vascular smooth muscle cell migration and apoptosis: a proteomic analysis. Cardiovasc. Res. **80**, 114–122 (2008)
41 Dudeck, A., Leist, M., Rubant, S., et al.: Immature mast cells exhibit rolling and adhesion to endothelial cells and subsequent diapedesis triggered by E- and P-selectin, VCAM-1 and PECAM-1. Exp. Dermatol. **19**(5), 424–434 (2010)
42 Shao, J.Y., Ting-Beall, H.P., Hochmuth R.M.: Staitic and dynamics lengths of neutrophil microvilli. PNAS **95**(12), 6797–6802 (1998)
43 Chen, S., Springer, T.A.: An automatic barking system that stabilizes leukocyte rolling by an increase in selectin bond number with shear. J. Cell Biol. **144**, 185–200 (1999)
44 Moore, K.L., Patel, K.D., Bruehl, R.E., et al.: P-selectin glycoprotein ligand-1 mediates rolling of human neutrophils on P-selectin. J. Cell Biol. **128**, 661–671 (1995)
45 Yago, T., Leppänen, A., Qiu, H., et al.: Distinct molecular and cellular contributions to stabilizing selectin-mediated rolling under flow. J. Cell Biol. **158**(4), 787–799 (2002)
46 Marshall, B.T., Sarangapani, K.K., Wu, J., et al.: Measuring molecular elasticity by atomic force microscope cantilever fluctuations. Biophys. J. **90**, 681–692 (2006)
47 Smith, M.J., Berg, E.L., Lawrence, M.B.: A direct comparison of selectinmediated transient, adhesive events using high temporal resolution. Biophys. J. **77**, 3371–3383 (1999)
48 Mehta, P., Cummings, R.D., McEver, R.P.: Affinity and kinetic analysis of P-selectin binding to P-selectin glycoprotein ligand-1. J. Biol. Chem. **273**, 32506–32513 (1998)